The Astrophysical Journal, 792:35 (8pp), 2014 September 1 doi:10.1088/0004-637X/792/1/35

NEW CONSTRAINTS ON COSMIC POLARIZATION ROTATION FROM *B*-MODE POLARIZATION IN THE COSMIC MICROWAVE BACKGROUND

Sperello di Serego Alighieri[1], Wei-Tou Ni[2], and Wei-Ping Pan[2]
[1] INAF—Osservatorio Astrofisico di Arcetri, Largo Enrico Fermi 5, I-50125 Firenze, Italy; sperello@arcetri.astro.it
[2] Department of Physics, National Tsing Hua University, Hsinchu, Taiwan 30013, Republic of China; weitou@gmail.com, d9722518@oz.nthu.edu.tw
Received 2014 April 17; accepted 2014 July 8; published 2014 August 12

ABSTRACT

SPTpol, POLARBEAR, and BICEP2 have recently measured the cosmic microwave background (CMB) *B*-mode polarization in various sky regions of several tens of square degrees and obtained BB power spectra in the multipole range 20–3000, detecting the components due to gravitational lensing and to inflationary gravitational waves. We analyze jointly the results of these three experiments and propose modifications to their analyses of the spectra to include in the model, in addition to the gravitational lensing and the inflationary gravitational wave components, and also the effects induced by the cosmic polarization rotation (CPR), if it exists within current upper limits. Although in principle our analysis would also lead to new constraints on CPR, in practice these can only be given on its fluctuations $\langle\delta\alpha^2\rangle$, since constraints on its mean angle are inhibited by the derotation which is applied by current CMB polarization experiments, in order to cope with the insufficient calibration of the polarization angle. The combined data fits from all three experiments (with 29% CPR–SPTpol correlation, depending on the theoretical model) gives the constraint $\langle\delta\alpha^2\rangle^{1/2} < 27.3$ mrad (1.°56), with $r = 0.194 \pm 0.033$. These results show that the present data are consistent with no CPR detection and the constraint on CPR fluctuation is about 1.°5. This method of constraining the CPR is new, is complementary to previous tests, which use the radio and optical/UV polarization of radio galaxies and the CMB *E*-mode polarization, and adds a new constraint for the sky areas observed by SPTpol, POLARBEAR, and BICEP2.

Key words: cosmic background radiation – cosmological parameters – early universe – gravitation – inflation – polarization

Online-only material: color figures

1. INTRODUCTION

The BICEP2 collaboration (Ade et al. 2014b) has recently detected the cosmic microwave background (CMB) *B*-mode (tensor mode) polarization and finds an excess power around $l \sim 80$ over the gravitational lensing expectation with a significance of more than 5σ, which they interpret as due to inflationary gravitational waves with a tensor-to-scalar ratio $r = 0.20^{+0.07}_{-0.05}$. This result is in apparent contrast with the limit previously set by the Planck collaboration $r < 0.11$ at 95% CL (Ade et al. 2014a). Three processes can produce *B*-mode polarization: (1) gravitational lensing from *E*-mode polarization (Zaldarriaga & Seljak 1997), (2) local quadrupole anisotropies in the CMB within the last scattering region by large scale gravitational waves (Polnarev 1985), and (3) cosmic polarization rotation (CPR)[3] due to pseudoscalar–photon interaction (Ni 1973; for a review, see Ni 2010). CPR is currently constrained to be less than about a couple of degrees by measurements of the linear polarization of radio galaxies and of the CMB (see di Serego Alighieri 2011 for a review). However, if CPR exists within the current upper limits, it would produce a non-negligible *B*-mode CMB polarization. The BICEP2 Collaboration (Ade et al. 2014b) has not considered this latter component in their model. To look for new constraints on the CPR and into the robustness of the BICEP2 fit, we include the CPR effect in the model. *TE*, *TB*, and *EB* correlations[4] potentially give mean values of the CPR angle $\langle\alpha\rangle$, while the contribution of CPR effects to the *B*-mode power potentially gives $\langle\alpha\rangle^2$ plus the variations of the CPR angle squared $\langle\delta\alpha^2\rangle$. This method of constraining the CPR is new, is complementary to previous tests, and adds a new constraint for the sky area observed, although its application to current data is limited by the uniform angle derotation, which is applied to the measured CMB *Q* and *U* maps to compensate for insufficient calibrations of the polarization angle (Keating et al. 2013). We also include in our analysis of the *B*-mode power spectra the data available for $l \geqslant 200$, in particular, from SPTpol (Hanson et al. 2013) and POLARBEAR (Ade et al. 2014c), in addition those from BICEP2 for $l \leqslant 335$.

In Section 2, we review the pseudoscalar–photon interaction, its modifications to the Maxwell equations, and the associated electromagnetic propagation effect on polarization rotation. In Section 3 we present the results of our fits. In Section 4 we review and discuss various constraints on CPR, and in Section 5 we discuss a few issues and present an outlook for the future.

2. PSEUDOSCALAR–PHOTON INTERACTION, MODIFIED PROPAGATION, AND POLARIZATION ROTATION

The Einstein equivalence principle (EEP) assumes local special relativity is a major cornerstone of general relativity and metric theories of gravity. Special relativity sprang from Maxwell–Lorentz electrodynamics. Maxwell equations in terms of field strength F_{kl} $(\boldsymbol{E}, \boldsymbol{B})$ and excitation H^{ij} $(\boldsymbol{D}, \boldsymbol{H})$ do not need metrics as a primitive concept. The field strength F_{kl} $(\boldsymbol{E}, \boldsymbol{B})$ and excitation H^{ij} $(\boldsymbol{D}, \boldsymbol{H})$ can all be independently defined operationally (e.g., Hehl & Obukhov 2003). To complete this set of equations, one needs the constitutive relation between the excitation and the field in both macroscopic electrodynamics

[3] The CPR has also been inappropriately called the cosmological birefringence, but we follow here the recommendation of Ni (2010).
[4] From sky maps of CMB temperature (T), *E*-mode polarization (E), and *B*-mode polarization (B), BB power spectra and *TE*, *TB*, and *EB* cross-correlations can be obtained as a function of the multipole *l*.

and in the spacetime theory of gravity:

$$H^{ij} = (1/2)\chi^{ijkl}F_{kl}. \quad (1)$$

When EEP is observed, this fundamental spacetime tensor density is induced by the metric g^{ij} of the form

$$\chi^{ijkl} = (1/2)(-g)^{1/2}(g^{ik}g^{jl} - g^{il}g^{kj}), \quad (g \equiv (\det g^{ij})^{-1}), \quad (2)$$

and the Maxwell equations can be derived from a Lagrangian density. In the local inertial frame, the spacetime tensor has the special relativity form (1/2) ($\eta^{ik}\,\eta^{jl} - \eta^{il}\,\eta^{kj}$), with η^{il} the Minkowski metric. To study the empirical foundation of EEP, it is crucial to explore how the experiments/observations constrain the general spacetime tensor χ^{ijkl} to the general relativity/metric form.

Since both H^{ij} and F_{kl} are antisymmetric, χ^{ijkl} must be antisymmetric in i and j, and k and l. Hence the constitutive tensor density χ^{ijkl} has 36 independent components, and can be decomposed into the principal part (P), axion part (Ax), and Hehl–Obukhov–Rubilar skewon part (Sk; Hehl & Obukhov 2003). The skewon ${}^{(\mathrm{Sk})}\chi^{ijkl}$ part is antisymmetric in the exchange of index pair ij and kl, satisfies a traceless condition, and has 15 independent components. The principal part and the axion (pseudoscalar) part constitute the parts that are symmetric in the exchange of the index pairs ij and kl. Together they have 21 independent components. The axion (pseudoscalar field) part is totally antisymmetric in all four indices and can be expressed as $\varphi\, e^{ijkl}$, with φ the pseudoscalar field and e^{ijkl} the completely antisymmetric Levi–Civita symbol. The principal part then has 20 degrees of freedom.

In constraining the general spacetime tensor from experiments and observations, we notice that EEP is already well tested and can only be violated weakly. Hence, one can start with Equation (2), adding a small general ${}^{(\mathrm{Sk})}\chi^{ijkl}$ to look for a constraint on skewons first. From the dispersion relation it is shown that no dissipation/no amplification in the propagation implies that the additional skewon field must be of type II (Ni 2014). For a type I skewon field, the dissipation/amplification in the propagation is proportional to the frequency and the CMB spectrum would deviate from the Planck spectrum. From the high precision agreement of the CMB spectrum with the 2.755 K Planck spectrum (Fixsen 2009), the type I cosmic skewon field $|{}^{(\mathrm{SkI})}\chi^{ijkl}|$ is constrained to less than a few parts of 10^{-35} (Ni 2014). A generic type II skewon field can be constructed from the antisymmetric part of an asymmetric metric and is allowed.

EEP implies that photons with the same initial position and direction follow the same world line and keep the same polarization state independent of energy (frequency) and polarization, i.e., no birefringence and no polarization rotation. This is observed to high precision for no birefringence and constrained for no polarization rotation. Since a type II skewon field in the weak-field limit and an axion (pseudoscalar) field do not contribute to the dispersion relation in the eikonal approximation (geometrical optics limit), the no-birefringence condition only limits the principal part of the spacetime tensor ${}^{(\mathrm{P})}\chi^{ijkl}$ to

$${}^{(\mathrm{P})}\chi^{ijkl} = 1/2(-h)^{1/2}[h^{ik}h^{jl} - h^{il}h^{kj}]\psi, \quad (3)$$

where the light cone metric h^{ik} can be expressed in terms of ${}^{(\mathrm{P})}\chi^{ijkl}$ and the Minkowski metric with $h \equiv (\det h^{ij})^{-1}$ (Ni 1983a, 1984). In the skewonless case, the no-birefringence condition is

$$\chi^{ijkl} = 1/2(-h)^{1/2}[h^{ik}h^{jl} - h^{il}h^{kj}]\psi + \varphi e^{ijkl}, \quad (4)$$

(Ni 1983a, 1984). Equation (4) has also been proved more recently without weak-field approximation for a non-birefringent medium in the skewonless case (Favaro & Bergamin 2011; Lämmerzahl & Hehl 2004). Polarization measurements of electromagnetic waves from pulsars and cosmologically distant astrophysical sources yield stringent constraints agreeing with Equation (4) down to 2×10^{-32} fractionally (for a review, see Ni 2010).

The constraint of the light cone metric h^{il} to the matter metric g^{il} up to a scalar factor can be obtained from Hughes–Drever-type experiments and the constraint on the dilaton ψ to 1 (constant) can be obtained from Eötvös-type experiments to high precision (Ni 1983a, 1983b, 1984).

We note that in looking for the empirical foundation of EEP above, only the axion field and type II skewon field are not well constrained. In Section 4, observational constraints on the pseudoscalar–photon interaction (axion field) are reviewed. These give an upper limit of a few degrees for the mean value part of the difference of the pseudoscalar field at the last scattering surface and at the observation point. In this paper, we look into further constraints/evidence of pseudoscalar–photon interaction in CMB B-mode polarization, especially on the fluctuation/variation part.

The interaction Lagrangian density for the pseudoscalar–photon interaction is

$$\begin{aligned} L_{\mathrm{I}}^{(\mathrm{EM-Ax})} &= -(1/(16\pi))\varphi\, e^{ijkl}F_{ij}\, F_{kl} \\ &= -(1/(4\pi))\,\varphi_{,i}e^{ijkl}A_j A_{k,l}(\text{mod div}), \end{aligned} \quad (5)$$

where "mod div" means that the two Lagrangian densities are related by integration by parts in the action integral (Ni 1973, 1974, 1977). If we assume that the φ term is local charge conjugation, parity inversion, and time reversal (CPT) invariant, then φ should be a pseudoscalar (function) since e^{ijkl} is a pseudotensor density. Note that sometimes one inserts a constant parameter to this term; here we absorb this parameter into the definition of the pseudoscalar field φ. The Maxwell equations (Ni 1973, 1977) become

$$F^{ik}_{;k} + (-g)^{-1/2}\mathrm{e}^{ikml}F_{km}\varphi_{,l} = 0, \quad (6)$$

where the derivation ";" is with respect to the Christoffel connection. The Lorentz force law is the same as in metric theories of gravity or general relativity. Gauge invariance and charge conservation are guaranteed. The modified Maxwell equations are conformal invariants also.

In a local inertial (Lorentz) frame of the g-metric, Equation (6) is reduced to

$$F^{ik}_{,k} + e^{ikml}F_{km}\varphi_{,l} = 0. \quad (7)$$

Analyzing the wave into Fourier components, imposing the radiation gauge condition, and solving the dispersion eigenvalue problem, we obtain $k = \omega + (n^{\mu}\varphi_{,\mu} + \varphi_{,0})$ for a right circularly polarized wave and $k = \omega - (n^{\mu}\varphi_{,\mu} + \varphi_{,0})$ for a left circularly polarized wave (Ni 1973; see Ni 2010 for a review). Here n^{μ} is the unit 3-vector in the propagation direction. The group velocity is independent of polarization:

$$v_g = \partial\omega/\partial k = 1. \quad (8)$$

There is no birefringence. This property is well known (Ni 1973, 1984; Hehl & Obukhov 2003; Itin 2013). For the right circularly polarized electromagnetic wave, the propagation from a point P_1 (4-point) to another point P_2 adds a phase of $\alpha = \varphi(\mathrm{P}_2) - \varphi(\mathrm{P}_1)$

to the wave; for the left circularly polarized light, the added phase will be opposite in sign (Ni 1973). Linearly polarized electromagnetic wave is a superposition of circularly polarized waves. Its polarization vector will then rotate by an angle α.

When we integrate along the light (wave) trajectory in a global situation, the total polarization rotation (relative to no φ interaction) is again $\alpha = \Delta\varphi = \varphi(\mathrm{P}_2) - \varphi(\mathrm{P}_1)$ since φ is a scalar field where $\varphi(\mathrm{P}_1)$ and $\varphi(\mathrm{P}_2)$ are the values of the scalar field at the beginning and end of the wave. When the propagation distance is over a large part of our observed universe, we call this phenomenon cosmic polarization rotation (Ni 2008).

In the CMB polarization observations, the variations and fluctuations due to pseudoscalar-modified propagation can be expressed as $\delta\varphi(\mathrm{P}_2) - \delta\varphi(\mathrm{P}_1)$, where $\delta\varphi(\mathrm{P}_1)$ is the variation/fluctuation at the last scattering surface. $\delta\varphi(\mathrm{P}_2)$ at the present observation point (fixed) is zero. Therefore, the covariance of the fluctuation $\langle[\delta\varphi(\mathrm{P}_2) - \delta\varphi(\mathrm{P}_1]^2\rangle$ is the covariance of $\delta\varphi^2(\mathrm{P}_1)$ at the last scattering surface. Since our universe is isotropic and homogeneous at the last scattering surface to $\sim 10^{-5}$, this covariance is $\sim(\xi \times 10^{-5})^2\varphi^2(\mathrm{P}_1)$, where the parameter ξ depends on various cosmological models (Ni 2008).

In the propagation, E-mode polarization will rotate into B-mode polarization with a $\sin^2 2\alpha$ ($\approx 4\alpha^2$ for small α) fraction of the power. For uniform rotation across the sky, the azimuthal eigenvalue l is invariant under polarization rotation and does not change. For small angles,

$$\alpha = \varphi(\mathrm{P}_2) - \varphi(\mathrm{P}_1) = [\varphi(\mathrm{P}_2) - \varphi(\mathrm{P}_1)]_{\mathrm{mean}} + \delta\varphi(\mathrm{P}_1) = \langle\alpha\rangle + \delta\alpha, \tag{9}$$

$$\underline{\alpha}^2 \equiv \langle\alpha^2\rangle = ([\varphi(\mathrm{P}_2) - \varphi(\mathrm{P}_1)]_{\mathrm{mean}})^2 + \langle\delta\varphi^2(\mathrm{P}_1)\rangle = \langle\alpha\rangle^2 + \langle\delta\alpha^2\rangle, \tag{10}$$

where $\underline{\alpha} \equiv \langle\alpha^2\rangle^{1/2}$ is the rms-sum polarization rotation angle, $[\varphi(\mathrm{P}_2) - \varphi(\mathrm{P}_1)]_{\mathrm{mean}} = \langle\alpha\rangle$ and $\delta\alpha = \delta\varphi(\mathrm{P}_1)$.

In translating the power distribution to the azimuthal eigenvalue variable l, we need to insert a factor $\zeta(l) \approx 1$ in front of $\delta_1\varphi^2(2)$ to take care of the nonlinear conversion to l due to fluctuations. For a uniform rotation with angle α across the sky, the rotation of the (original) E-mode power C_l^{EE} into the B-mode power $C_l^{BB,\mathrm{obs}}$ and EB correlation power is given by (see, e.g., Keating et al. 2013):

$$C_l^{BB,\mathrm{obs}} = C_l^{BB}\cos^2(2\alpha) + C_l^{EE}\sin^2(2\alpha), \tag{11a}$$

$$C_l^{EB,\mathrm{obs}} = \left(C_l^{EE} - C_l^{BB}\right)\ \sin\,(2\alpha)\ \cos\,(2\alpha). \tag{11b}$$

The rotation of the (original) B-mode power C_l^{BB} into the E-mode power $C_l^{EE,\mathrm{obs}}$ and EB correlation power is small and negligible in our analysis since the primordial B-mode is small compared with the E-mode power. For CPR fluctuation in a patch of sky, if we consider only the components deriving from the E-mode power C_l^{EE} for $l > 20$, the rotated-part B-mode l-power spectrum $C_l^{BB,\mathrm{obs}}$ and the rotated EB correlation power $C_l^{EB,\mathrm{obs}}$ for a small CPR angle $\underline{\alpha}$ is accurately given by

$$C_l^{BB,\mathrm{obs}} \approx C_l^{EE}\ \sin^2(2\alpha) \approx 4\underline{\alpha}^2\ C_l^{EE}, \tag{12a}$$

$$C_l^{EB,\mathrm{obs}} \approx C_l^{EE}\ \sin(2\alpha)\ \cos\,(2\alpha) \approx 2\langle\alpha\rangle\ C_l^{EE}. \tag{12b}$$

The accuracy of Equation (12a) is shown in Figure 1, which compares the E-mode power spectrum from Figure 10 of Lewis & Challinor (2006) and the CPR B-mode power spectrum from Figure 5 of Zhao & Li (2014). They are almost identical up to a scale $4\underline{\alpha}^2$ although their input parameters are slightly different.

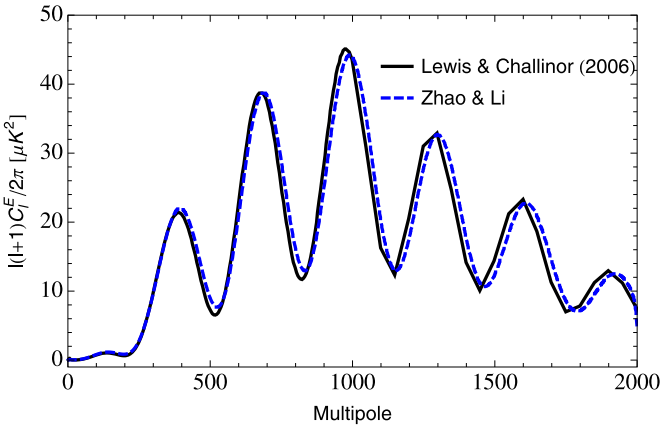

Figure 1. Comparison of the E-mode power spectrum from Figure 10 of Lewis & Challinor (2006) and the CPR B-mode power spectrum from Figure 5 of Zhao & Li (2014) up to a scale of $4\underline{\alpha}^2$.

(A color version of this figure is available in the online journal.)

The present BICEP2 data group about 32 azimuthal eigenmodes into one band, with the lowest l contribution greater than 20; $\zeta(l)$ is virtually equal to one. We will set it to one in our analysis. For precise measurement of variations/fluctuations, direct processing of data without first evaluating the l components may be an alternative method.

Some CMB polarization projects apply a uniform angle derotation to the measured Q and U maps by minimizing the TB and EB power to compensate for insufficient calibrations of the polarization angle (Keating et al. 2013). This procedure will automatically eliminate the sum of any systematic error in the polarization angle calibration and of any uniform CPR, if it exists. If calibration errors of the polarization angle were small compared to the uniform CPR, in principle this minimization procedure could provide an estimate of the uniform CPR angle $\langle\alpha\rangle$. However, since the systematic errors in the polarization angle are of the same order as current upper limits to uniform CPR, this procedure in fact is equivalent to assuming no uniform CPR and will preclude any information on it.

SPTpol first estimates the lensing potential from a *Herschel*-SPERE map of the cosmic infrared background and constructs a template for the lensing B-mode signal by combining the SPTpol-measured E-mode polarization with the estimated lensing potential. SPTpol then compares this constructed template to its directly measured B-modes to determine the lensing B-mode by correlation method. In this way the uniform (mean) CPR would not be included. The CPR fluctuations incurred at the lensing site would be included and correlated with the pseudoscalar fluctuations at the lensing site ($z \sim 2$–5). Assuming that the linear perturbation scheme works, the uniform (mean) part of the pseudoscalar field at lensing is developed from the uniform (mean) part of the pseudoscalar field at the last scattering surface, and the pseudoscalar fluctuations at lensing are also developed from the fluctuations at the last scattering surface ($z \sim 1100$). In most theoretical models, the pseudoscalar fluctuations are correlated to the density fluctuations at the last scattering surface. Therefore, the pseudoscalar field fluctuations at lensing would also be correlated with density fluctuations at lensing. The strength of this correlation depends on cosmological models with a pseudoscalar field. Effects from re-ionization are minor but could also be included. Therefore, in the fits with

Table 1
Results of Fitting the CPR Fluctuation $\delta\alpha^2$ and/or the Scalar-to-tensor Ratio r to BICEP2 (Ade et al. 2014b), POLARBEAR (Ade et al. 2014c), and SPTpol (Hanson et al. 2013), and Their Joint Combinations

Experiment	Fitting Parameter		$\chi_{\rm min}{}^2$ (No. of Data Points − No. of Fitting Parameters)	1σ Upper Limit on CPR Fluctuation Amplitude $\langle\delta\alpha^2\rangle^{1/2}$ (mrad)
	$\langle\delta\alpha^2\rangle$ (mrad^2)	r		
BICEP2	339 ± 455	0.196 ± 0.033	10.424 (9 – 2)	28.2 (1.°61)
POLARBEAR	89 ± 535	0.2[a]	3.73 (4 – 1)	25.0 (1.°43)
POLARBEAR + BICEP2	265 ± 397	0.198 ± 0.033	14.31 (13 – 2)	25.7 (1.°47)
SPTpol	$\kappa^{-1}(233 \pm 148)$	0.2[a]	2.61 (4 – 1)	κ^{-1}19.5 (κ^{-1}1.°12)
SPTpol (23%) + BICEP2	486 ± 411	0.190 ± 0.033	13.81 (13 – 2)	29.9 (1.°72)
SPTpol (70%) + BICEP2	340 ± 270	0.196 ± 0.033	13.05 (13 – 2)	24.7 (1.°42)
SPTpol (100%) + BICEP2	244 ± 202	0.199 ± 0.033	13.13 (13 – 2)	21.1 (1.°21)
POLARBEAR + BICEP2 + SPTpol (29%)	392 ± 353	0.194 ± 0.033	19.27 (17 – 2)	27.3 (1.°56)
POLARBEAR + BICEP2 + SPTpol (86%)	264 ± 218	0.198 ± 0.033	18.34 (17 – 2)	22.0 (1.°26)

Note. [a] r is set to 0.2 to conform to BICEP2 data; the effect of setting r to 0.2 or 0 to the CPR fluctuation fitting is small since the power of a non-vanishing r contribution to the total power is small for the multipoles measured in the POLARBEAR and SPTpol experiments.

SPTpol data, we include a percentage correlation parameter κ (this parameter could also be greater than one in some models).

3. MODELING THE DATA

In this section, we model the available data for the BB power spectrum with the three effects mentioned in the Introduction. The theoretical spectrum of the inflationary gravitational waves and the lensing contribution to B-mode are extracted from the BICEP2 paper (Ade et al. 2014b). The power spectrum $C_l^{BB,\rm obs}$, induced by any existing CPR angle (Equation (12a)), is obtained from the theoretical E-mode power spectrum C_l^{EE} of Lewis & Challinor (2006) and is shown in Figure 1.

The data on the BB power spectrum are the nine points of BICEP2 in Figure 14 of Ade et al. (2014b) for the low multipole part ($21 \leqslant l \leqslant 335$), the four points of SPTpol in Figure 2 of Hanson et al. (2013) for $200 \leqslant l \leqslant 3000$, and the four points of POLARBEAR (Ade et al. 2014c) for $500 \leqslant l \leqslant 2100$, based on observations at 150 GHz on three regions of the sky for a total of 30 deg^2. Although the signal-to-noise ratio of the recently published results of POLARBEAR for the CMB B-mode polarization is considerably lower than that obtained by the SPTpol collaboration in the same range of l, the SPTpol data, depending on theoretical models, only include CPR partially in their lensing correlation measurement. Therefore, we have considered both data sets in our fits. As it turned out, the three experiments give similar constraints on the relevant CPR parameters.

Since a uniform derotation is implemented by both the BICEP2 and POLARBEAR experiments, by minimizing the EB and TB power to compensate for the relatively large errors in the calibration of the polarization angle, their data can only give constraints on the CPR fluctuations (variance), but not on the CPR mean angle. SPTpol have not applied such a derotation, although their systematic uncertainty on the polarization angle is about 1° at 150 GHz. However, they give the cross-correlation of their measured B-modes with the lensing B-modes inferred from cosmic infrared background fluctuations as measured by *Herschel*, rather than the BB autocorrelation. Therefore, also from the SPTpol data, it is possible to derive a constraint only on the CPR fluctuations, not on the mean angle.

Table 1 and Figures 2–7 show the results of our fits for various combinations of the available data and for different values of the correlation percentage κ of the pseudoscalar field fluctuations with the density fluctuations at lensing in the SPTpol case.

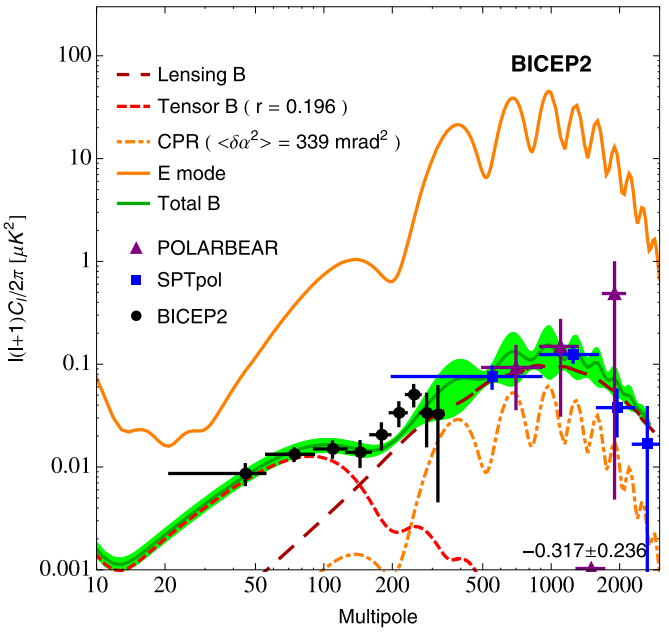

Figure 2. B-mode spectrum showing the best fit (dark green line) and the 1σ region (green band) to the nine BICEP2 data points (black filled circles), with the vertical bar showing the standard deviation of each data point and the horizontal bar showing the binning interval. The E-mode is plotted for reference. The power of the second highest multipole band of POLARBEAR (l from 1300 to 1700) is negative, i.e., -0.317 ± 0.236 μK^2; we show the binning interval on the horizontal axis with the data value in Arabic numerals above the binning interval.

(A color version of this figure is available in the online journal.)

Figure 2 shows the results of the fitting of the CPR fluctuation and of the scalar-to-tensor ratio for BICEP2. Figure 3 shows the results of the fitting to the POLARBEAR experiment. Figure 4 shows the results of the joint fitting to BICEP2 and POLARBEAR. Figure 5 shows the results of the fitting to the SPTpol experiment. Figure 6 shows the joint BICEP2–SPTpol fitting and Figure 7 the joint BICEP2–POLARBEAR–SPTpol fitting. Figure 6(b) shows how the χ^2 and the CPR angle fluctuations vary with the CPR–SPTpol correlation percentage κ, considering BICEP2 and SPTpol data: the minimum χ^2 is obtained at 70% (but it is a shallow minimum) and the largest CPR fluctuations are obtained at 23%. Figure 7(b) show the same for all three experiments: in this case the minimum χ^2 is obtained at 86% and the largest CPR variance is at 29%.

Table 2
Recent Constraints on Uniform CPR Angle from CMB *E*-mode Polarization

Experiment	Frequencies	*l*-range	CPR Angle	Reference
*WMAP*9	41, 61,94 GHz	2–800	$-0.^{\circ}36 \pm 1.^{\circ}24 \pm 1.^{\circ}5$	Hinshaw et al. (2013)
BICEP1	100,150 GHz	20–335	$-2.^{\circ}77 \pm 0.^{\circ}86 \pm 1.^{\circ}3$	Kaufman et al. (2014)

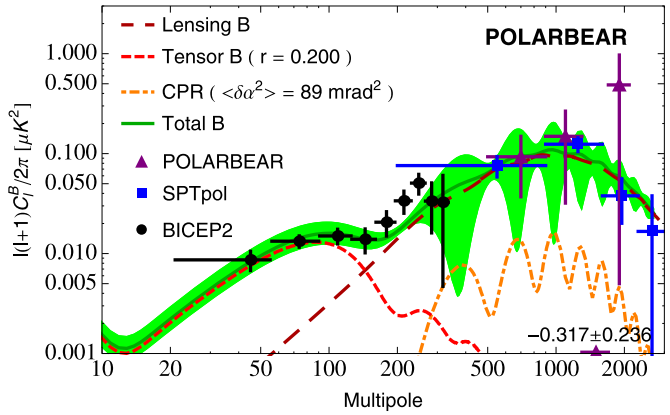

Figure 3. Same as Figure 2, but for the POLARBEAR data points (purple filled triangle). r is set to 0.2 to conform to BICEP2 data; the effect of setting r to 0.2 or to 0 for the fitting of the CPR fluctuation is small since the power contributed by a non-vanishing r to the total power is small for the multipoles measured in the POLARBEAR experiment.

(A color version of this figure is available in the online journal.)

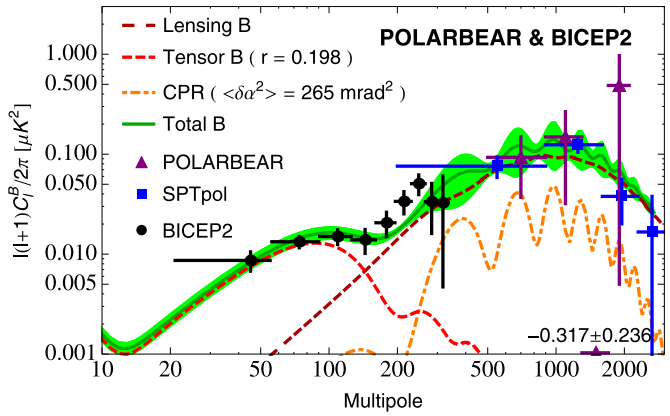

Figure 4. Same as Figure 2, but for the BICEP2 (black filled circles) and POLARBEAR data points (purple filled triangle).

(A color version of this figure is available in the online journal.)

4. CONSTRAINTS ON COSMIC POLARIZATION ROTATION

The CPR has not yet been detected. Upper limits have been obtained from radio galaxy polarization, both in the radio and in the optical/UV (di Serego Alighieri et al. 2010), and from CMB polarization anisotropies. These limits were reviewed by di Serego Alighieri (2011): all methods have reached an accuracy of about 1° and 3σ upper limits to any rotation of a few degrees. Since this review, only minor revisions of the limits from the CMB have appeared (see Table 2). Gluscevic et al. (2012) searched for direction-dependent CPRs with *Wilkinson Microwave Anisotropy Probe* (*WMAP*) 7 yr data and obtained an upper limit on the rms rotation angle $\langle\alpha^2\rangle^{1/2} < 9.^{\circ}5$ for $0 < l < 512$ and an upper limit at 68% CL of about 1° on the quadrupole of a scale-independent rotation-angle power spectrum.

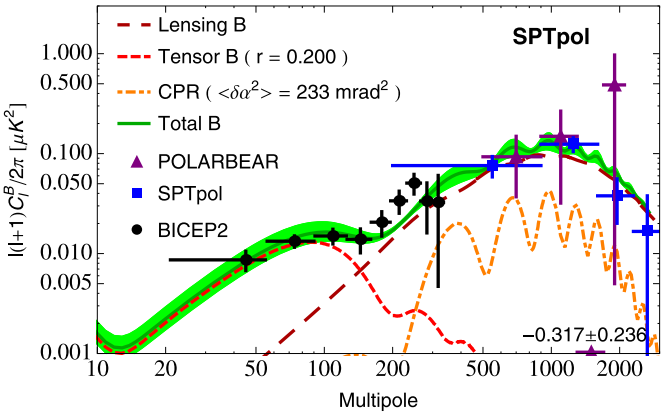

Figure 5. Same as Figure 2, but for the SPTpol data points (blue filled square) with 100% CPR–SPTpol correlation. This is a one-parameter fit to the CPR effect. For theoretical models with CPR–SPTpol correlation κ, the fitted value of $\langle\delta\alpha^2\rangle$ is $\kappa^{-1}(233 \pm 148)$ mrad^2 instead. r is set to 0.2 to conform to BICEP2 data; the effect of setting r to 0.2 or to 0 for the fitting of the CPR fluctuation is small since the power contribution of a non-vanishing r to the total power is small for the multipoles measured in the SPTpol experiment.

(A color version of this figure is available in the online journal.)

The rotation angle given by the revision of BICEP1 data by Kaufman et al. (2014) formally corresponds to a 1.78σ detection of CPR. However, taking into account the uncertainties involved in the calibration of the BICEP1 polarization angle, the problems in correcting for galactic Faraday rotation (Section VI.B of Kaufman et al. 2014), and the inconsistency of this result with the result of QUaD, for which Brown et al. (2009) give a CPR angle of $0.^{\circ}64 \pm 0.^{\circ}5$(stat.) $\pm 0.^{\circ}5$(syst.), we do not consider this CPR "detection" as final. Recently, Gubitosi & Paci (2013) have reviewed the constraints on CPR, but they considered only those derived from CMB polarization data.

By modeling the SPTpol, POLARBEAR, and BICEP2 data on the *B*-mode polarization power spectrum, taking into account the inflationary gravitational waves, the gravitational lensing, and the component induced by CPR, as explained in the previous sections, we can derive a new constraint on CPR fluctuations, since the present data limit $\langle\delta\alpha^2\rangle$. In fact in our case, since we cannot predict which should be the correlation percentage between the lensing *E*-mode and *B*-mode CPR effects, the most conservative CPR constraint is set at the percentage that gives the maximum $\langle\delta\alpha^2\rangle$, i.e., 29% (Figure 7(b) and upper part of Figure 7(a)). In fact, we also cannot consider instead the correlation percentage giving the lowest χ^2, i.e., 86% (Figure 7(b) and lower part of Figure 7(a)) because all correlation percentages between 30% and 100% give χ^2 values within 10% of the best one, hence they all are statistically acceptable. Therefore, using the data from the three available experiments, we can set a limit: $\langle\delta\alpha^2\rangle \leqslant 392{+}353 = 745$ mrad^2, i.e., $\langle\delta\alpha^2\rangle^{1/2} \leqslant 27.3$ mrad or $1.^{\circ}56$ at 68% C.L.

Our models give a value for r which is slightly lower than the value given by the BICEP2 collaboration (Ade et al. 2014b), but still in disagreement with the Planck six-parameter-fit limit (Ade et al. 2014a). However, the Planck limit is relaxed to $r <$

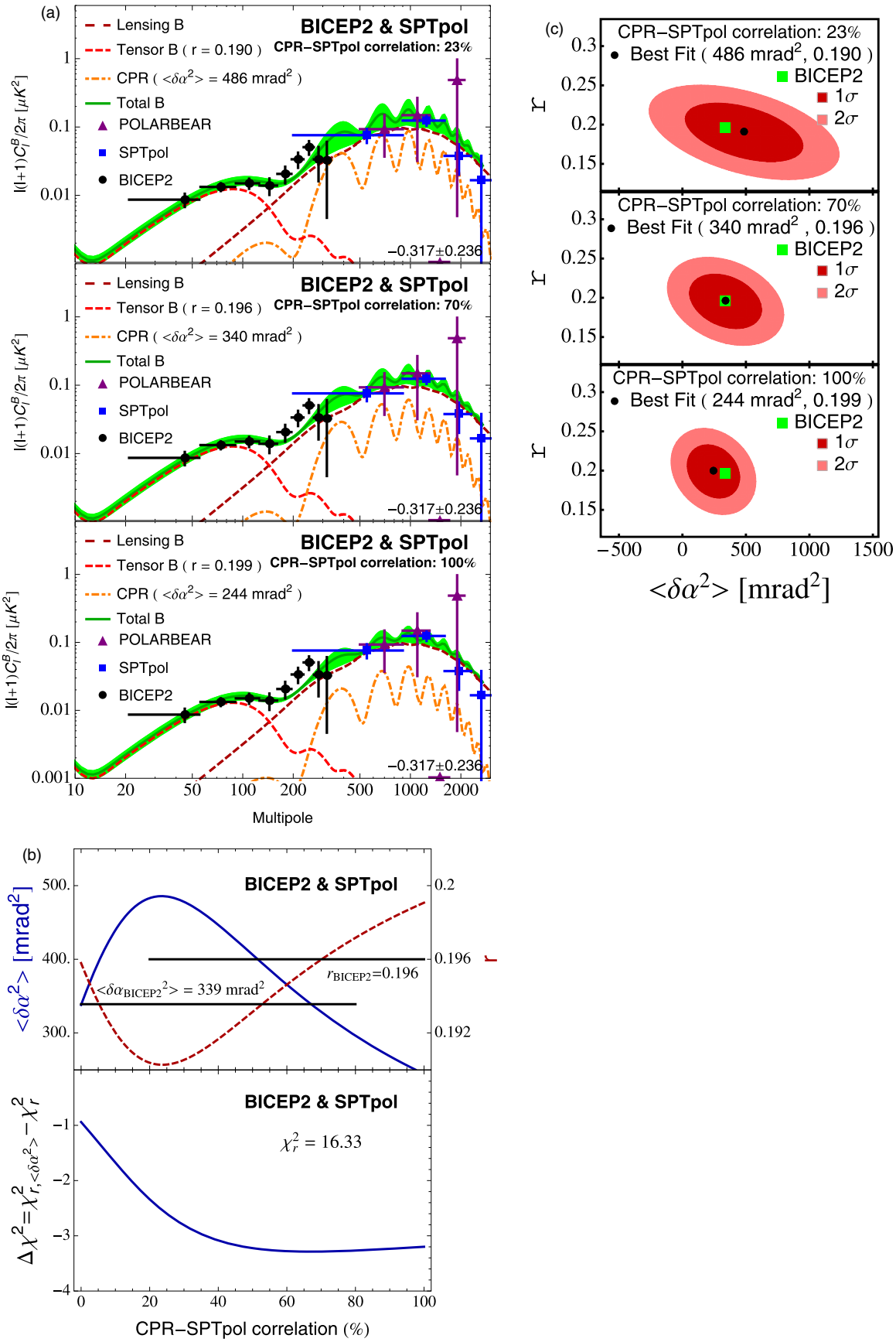

Figure 6. Panel (a) is the same as Figure 5, but for the BICEP2 data points (black filled circles) and SPTpol data points (blue filled square) with 23%, 70%, and 100% CPR–SPTpol correlations for the upper part, the middle part, and the lower part of figure, respectively. Panel (b) shows the dependence of $\langle\alpha\rangle^2$, r, and χ^2 on the CPR–SPTpol correlation κ; panel (c) shows the 1σ and 2σ contours of the joint constraint on the tensor-to-scalar ratio r and the rms sum of the CPR angle due to pseudoscalar–photon interaction for three cases in panel (a).

(A color version of this figure is available in the online journal.)

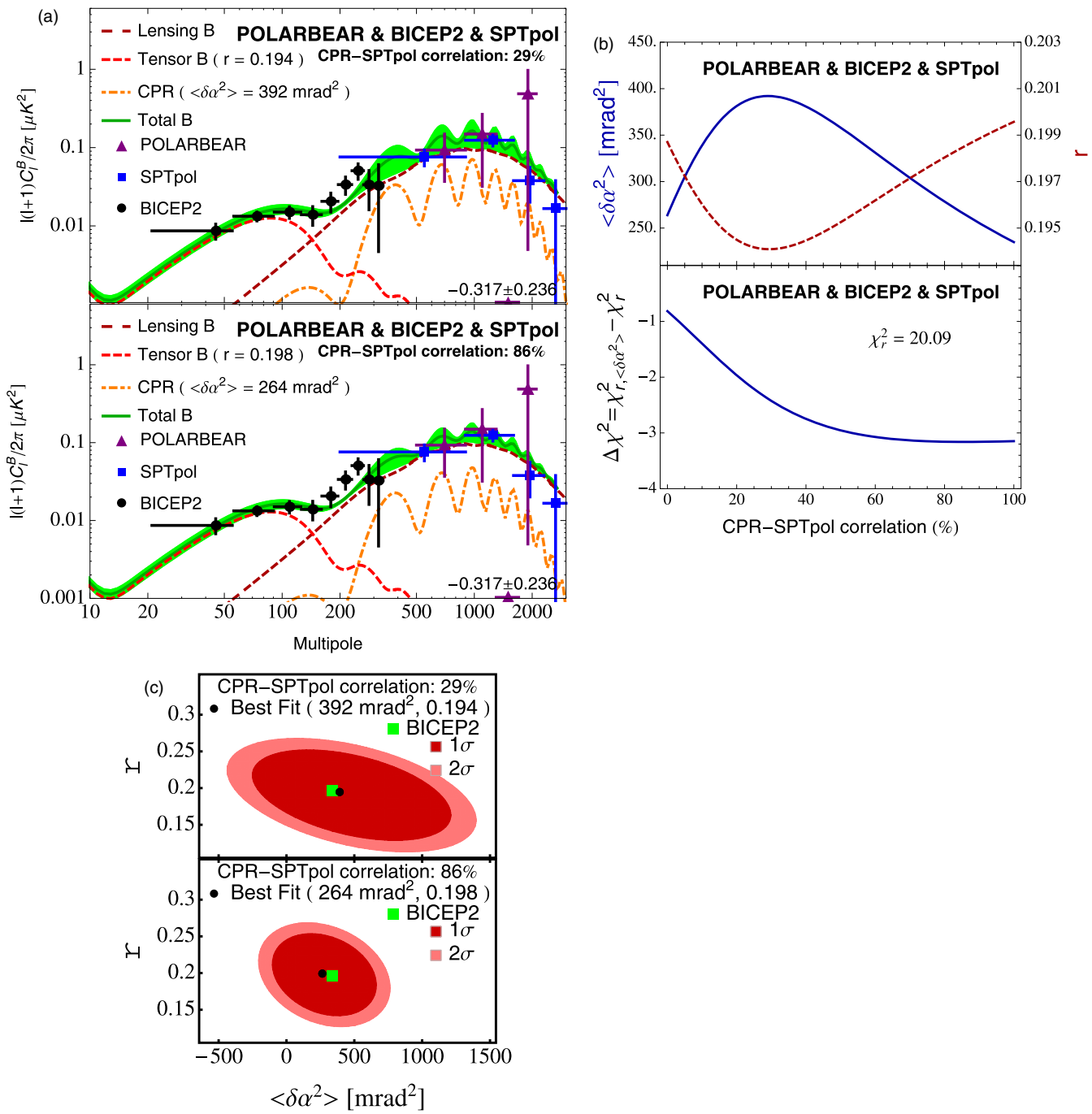

Figure 7. Panel (a) is the same as Figure 5, but for the BICEP2 data points (black filled circles), POLARBEAR data points (purple filled triangle), and SPTpol data points (purple filled triangle) with 29% and 86% CPR–SPTpol correlations for the upper part and the lower part of figure, respectively. Panel (b) shows the dependence of $\langle\alpha\rangle^2$, r, and χ^2 on the CPR–SPTpol correlation κ. Panel (c) shows the 1σ and 2σ contours of the joint constraint on the tensor-to-scalar ratio r and the rms sum of the CPR angle due to pseudoscalar–photon interaction for the two cases (panel (a)).

(A color version of this figure is available in the online journal.)

0.26 when running is allowed with $dn_s/d\ln k = -0.022 \pm 0.010$ (Ade et al. 2014b). Our fitted r value gives a 6σ detection, which agrees with the BICEP2 results and shows robustness to adding CPR effects.

Lee et al. (2014) recently modeled the power spectrum of the B-mode CMB polarization, including a component derived from the CPR (they call it "cosmological birefringence"), therefore decreasing the "primordial" component and bring it within the limit $r < 0.11$ set by Ade et al. (2014a). However, they considered only the BICEP2 data (Ade et al. 2014b) at low l, not the SPTpol nor POLARBEAR data (Hanson et al. 2013; Ade et al. 2014c) at high l, which together better constrain the CPR. Therefore, they allow for a much larger CPR component than we do. We believe that our approach is a considerable improvement.

5. DISCUSSION AND OUTLOOK

In this paper, we investigated, both theoretically and experimentally, the possibility of detecting CPR or setting new constraints on it, using its coupling with the B-mode power spectra of the CMB. Three experiments have detected B-mode

polarization in the CMB: SPTpol (Hanson et al. 2013) for $200 \leqslant l \leqslant 3000$, BICEP2 (Ade et al. 2014b) for $21 \leqslant l \leqslant 335$, and POLARBEAR (Ade et al. 2014c) for $500 \leqslant 1 \leqslant 2100$.

The practical realization of our suggestion has a problem: as explained in Section 3, currently available data on *B*-mode CMB polarization only allow the fluctuations of the CPR angle to be constrained, not its mean value. Using all available data we set a constraint to the fluctuations of the CPR: $\langle \delta\alpha^2 \rangle^{1/2} \leqslant 27.3$ mrad (1°.56) at 68% CL.

However, we believe that the method of investigating the CPR from data on the *B*-mode CMB polarization will become useful with future experiments, which will solve the problem of calibrating the polarization angle. For example, Naess et al. (2014) very recently reported a new measurement of the polarization of the Crab Nebula, an important calibration source, at 146 GHz with the Atacama Cosmology Telescope, giving an accuracy of 0°.5 on the angle, an improvement over previous measurements. Concerning the prospects for improvements in the detection/constraints on CPR in the near future, the *Planck* satellite (http://www.rssd.esa.int/index.php?project=Planck) is expected to allow for a considerable step forward, since it will have a sensitivity to polarization rotation on the order of a tenth of a degree and systematic errors of the same order (Gruppuso et al. 2012), provided that calibration procedures of sufficient accuracy for the polarization orientation are implemented. In any case the *Planck* polarization results are foreseen only toward the end of this year. Also, the Keck Array, which is a set of five telescopes very similar to the BICEP2 one, is expected to bring considerable improvements to current CMB polarization measurements. Three of these telescopes are already operating and results are expected soon, particularly for *B*-mode polarization due to inflationary gravitational waves (Pryke & BICEP2 and Keck-Array Collaborations 2013).

As far as we are aware, there is no current plan for extending the optical/UV polarization measurement of distant radio galaxies to a level that would bring considerable improvements on the CPR constraints obtained so far from these objects. However, it would be desirable to perform detailed spatially resolved observations of the optical/UV polarization of a few radio galaxies, of the kind performed on 3C 265 (Wardle et al. 1997), and selected to be in the sky areas also observed by CMB polarization experiments on the ground. In fact these observations are likely to constrain the CPR angle with an accuracy of better than 1°, thereby providing a better calibration for the absolute polarization angle than available so far to these experiments.

If pseudoscalar–photon interactions exist, a natural cosmic variation of the pseudoscalar field at the decoupling era is 10^{-5} fractionally. The CPR fluctuation is then of the order of $10^{-5}\varphi_{\text{decoupling-era}}$. We will search for the possibility of its detection or for more constraints in future experiments.

We thank Brian Keating and the referee for useful comments and Matteo Galaverni for useful discussion. W.T.N. would also like to thank the National Science Council (grant Nos. NSC101–2112-M-007–007 and NSC102–2112-M-007–019) and the National Center for Theoretical Sciences (NCTS) for supporting this work in part.

REFERENCES

Ade, P. A. R., Aghanim, N., Armitage-Caplan, C., et al. (Planck Collaboration) 2014a, A&A, in press (arXiv:1303.5076)
Ade, P. A. R., Aikin, R. W., Barkats, D., et al. (BICEP2 Collaboration) 2014b, PhRvL, 112, 241101
Ade, P. A. R., Akiba, Y., Anthony, A. E., et al. (POLARBEAR Collaboration) 2014c, arXiv:1403.2369
Brown, M. L., Ade, P., Bock, J., et al. (QUaD Collaboration) 2009, ApJ, 705, 978
di Serego Alighieri, S. 2011, in From Varying Couplings to Fundamental Physics, ed. C. Martins & P. Molaro (ASSP; Berlin: Springer), 139
di Serego Alighieri, S., Finelli, F., & Galaverni, M. 2010, ApJ, 715, 33
Favaro, A., & Bergamin, L. 2011, AnP, 523, 383
Fixsen, D. J. 2009, ApJ, 707, 916
Gluscevic, V., Hanson, D., Kamionkowski, M., & Hirata, C. M. 2012, PhRvD, 86, 103529
Gruppuso, A., Natoli, P., Mandolesi, N., et al. 2012, JCAP, 02, 023
Gubitosi, G., & Paci, F. 2013, JCAP, 02, 020
Hanson, D., Hoover, S., Crites, A., et al. (SPTpol Collaboration) 2013, PhRvL, 111, 141301
Hehl, F. W., & Obukhov, Y. N. 2003, Foundations of Classical Electrodynamics: Charge, Flux, and Metric (Boston, MA: Birkhäuser)
Hinshaw, G., Larson, D., Komatsu, E., et al. (WMAP Collaboration) 2013, ApJS, 208, 19
Itin, Y. 2013, PhRvD, 88, 107502
Kaufman, J. P., Miller, N. J., Shimon, M., et al. (BICEP1 Collaboration) 2014, PhRvD, 89, 062006
Keating, B. G., Shimon, M., & Yadav, A. P. S. 2013, ApJL, 762, L23
Lämmerzahl, C., & Hehl, F. W. 2004, PhRvD, 70, 105022
Lee, S., Liu, G.-C., & Ng, K.-W. 2014, arXiv:1403.5585
Lewis, A., & Challinor, A. 2006, PhR, 429, 1
Naess, S., Hasselfield, M., McMahon, J., et al. 2014, arXiv:1405.5524
Ni, W.-T. 1973, A Nonmetric Theory of Gravity (Bozeman, MT: Montana State Univ.), http://astrod.wikispaces.com/
Ni, W.-T. 1974, Bull. Am. Phys. Soc., 19, 655
Ni, W.-T. 1977, PhRvL, 38, 301
Ni, W.-T. (ed.) 1983a, in Proceedings of the 1983 International School and Symposium on Precision Measurement and Gravity Experiment (Hsinchu, Taiwan, Republic of China: National Tsing Hua University), 491 (http://astrod.wikispaces.com/)
Ni, W.-T. (ed.) 1983b, in Proceedings of the 1983 International School and Symposium on Precision Measurement and Gravity Experiment (Hsinchu, Taiwan, Republic of China: National Tsing Hua University), 519 (http://astrod.wikispaces.com/)
Ni, W.-T. 1984, in Precision Measurement and Fundamental Constants II, ed. B. N. Taylor & W. D. Phillips (Natl. Bur. Stand. Spec. Publ. 617; Washington, DC: U.S. Government Printing Office), 647
Ni, W.-T. 2008, PThPS, 172, 49
Ni, W.-T. 2010, RPPh, 73, 056901
Ni, W.-T. 2014, PhLA, 378, 1217
Polnarev, A. G. 1985, SvA, 29, 607
Pryke, C., & BICEP2 and Keck-Array Collaborations, 2013, in IAU Symp. 288, Astrophysics from Antartica, Vol. 8, ed. T. Montmerle, I. F. Corbett, U. Grothkopf, & C. Sterken (Cambridge: Cambridge Univ. Press), 68
Wardle, J. F. C., Perley, R. A., & Cohen, M. H. 1997, PhRvL, 79, 1801
Zaldarriaga, M., & Seljak, U. 1997, PhRvD, 55, 18309
Zhao, W., & Li, M. 2014, PhRvD, 89, 103518